Effect of native defects and laser-induced defects on multi-shot laser-induced damage in multilayer mirrors

Ying Wang (王 营)[1,2*], Yuanan Zhao (赵元安)[1], Jianda Shao (邵建达)[1], and Zhengxiu Fan (范正修)[1]

[1]*Key Laboratory of Materials for High Power Lasers, Shanghai Institute of Optics and Fine Mechanics, Chinese Academy of Science, Shanghai 201800, China*

[2]*Graduate University of Chinese Academy of Sciences, Beijing 100049, China*

[*]*Corresponding author: wangying@siom.ac.cn*

Received February 17, 2011; accepted April 14, 2011; posted online July 11, 2011

The roles of laser-induced defects and native defects in multilayer mirrors under multi-shot irradiation condition are investigated. The HfO_2/SiO_2 dielectric mirrors are deposited by electron beam evaporation (EBE). Laser damage testing is carried out on both the 1-on-1 and S-on-1 regimes using 355-nm pulsed laser at a duration of 8 ns. It is found that the single-shot laser-induced damage threshold (LIDT) is much higher than the multi-shot LIDT. In the multi-shot mode, the main factor influencing LIDT is the accumulation of irreversible laser-induced defects and native defects. The surface morphologies of the samples are observed by optical microscopy. Moreover, the number of laser-induced defects affects the damage probability of the samples. A correlative model based on critical conduction band (CB) electron density (ED) is presented to simulate the multi-shot damage behavior.

OCIS codes: 310.0310, 140.3330.

doi: 10.3788/COL201109.093102.

It is widely regarded that multi-shot laser-induced damage threshold (LIDT) in most optical materials decreases with increasing pulse number because of the accumulation effects[1−3]. Recently, many laboratories have investigated the multi-shot laser-induced damage (LID) of optical materials, such as fused silica[3] and KTP crystal[4]. Optical coatings are used very often in high-power laser systems[5]. As a result, the investigation of multi-shot LID of optical coatings is of high practical importance for high-power laser applications in recent years[6]. In a previous study, a model was developed to explain the correlations between the observed multi-shot LIDT and its dependence on the number of shots at 1 064 nm[7]. It is easier to generate the color center at an intensity below the damage threshold ultraviolet laser light[8]. The damage behavior of 355 nm is much complicated than that of 1 064 nm. The aim of this letter is to analyze the accumulation effect on laser damage resistance at 355 nm. The effect of native defects and laser induce defects on multi-shot LIDT is discussed.

The 355 high reflectivity (HR) coatings were prepared by electron beam evaporation (EBE). The coating design of the sample was $(HL)^{14}H$, where H and L stand for the high-index material (HfO_2) and the low-index material (SiO_2), respectively, with one-quarter wavelength optical thickness (QWOT).

The experimental setup for laser damage is shown schematically in Fig. 1, in which the Nd:YAG laser system is operated at the TEM_{00} mode and the pulse width is 8 ns at 355 nm. The beams were focused to a $1/e^2$ height of 380 μm and width of 350 μm. In the S-on-1 test, the sample was tested at the frequency of 5 Hz. The laser energy that was used to damage the sample was obtained by the adjustment of the attenuator, and the pulse energy was measured by an energy meter from a split-off portion of the beam. The sample was set upon a two-dimensional precision stage driven by a stepper motor. The He-Ne laser was used to monitor the test. Damage onset was detected online by a video microscopy system.

The S-on-1 test was carried out according to ISO 11254-2[9]. In this letter, 1-on-1, 5-on-1, 10-on-1, 20-on-1, and 100-on-1 LIDTs were tested to understand the influence of the shot number on the accumulation effects.

Two representations of the damage data can be found in Fig. 2. The S-on-1 damage probability curves with S ranging from 1 to 100 are shown in Fig. 2(a). The 0% damage probability is summarized in Fig. 2(b). The accumulation effects become clear in the two representations.

The data in Fig. 2(a) show the increase in damage probability with the number of pulses and a clear decrease in the damage threshold with the increase in laser pulse number. From Fig. 2(b), it can be seen that the 0% damage probability drops monotonically to a minimum value.

The damage morphology of the HR coatings was accessed by optical microscope. The typical damage morphology information after 1-on-1 and S-on-1 tests are shown in Fig. 3. All the morphologies clearly permit that the damages originated from small defects. The delamination characteristic of optical films can be seen in the S-on-1 test.

Due to interference effects in film, local intensity enhancements exist in the sample coatings. The theoretical

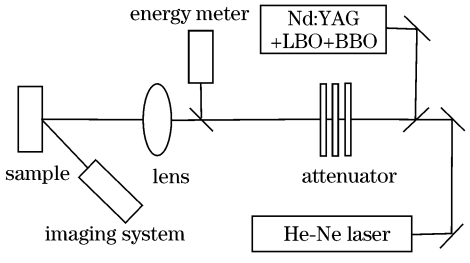

Fig. 1. Experimental setup of laser damage testing.

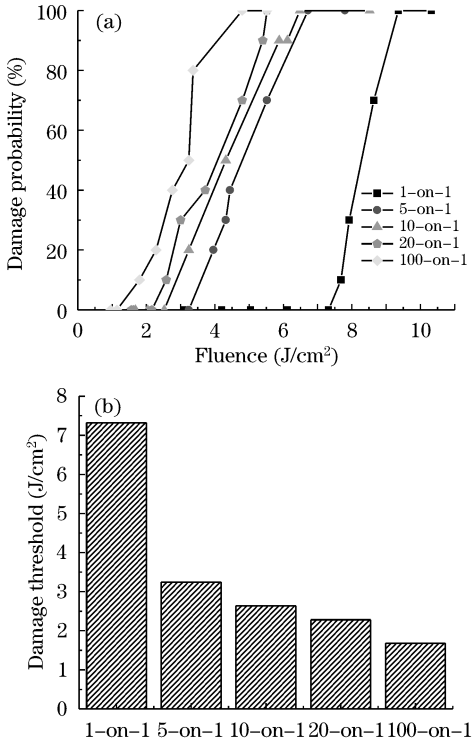

Fig. 2. (a) S-on-1 damage probability curves (S = 1, 5, 10, 20, and 100); (b) LIDT as a function of pulse number S.

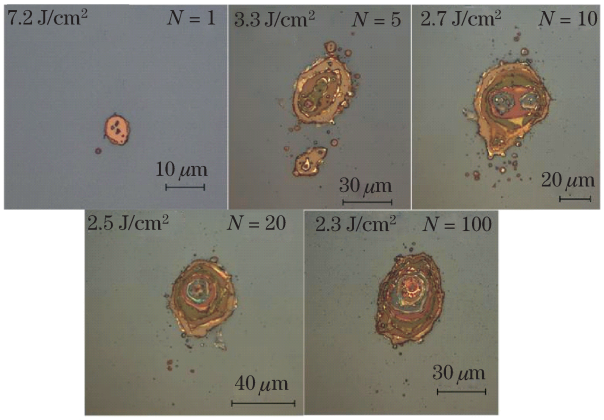

Fig. 3. Damage morphologies of the HR coatings.

results of electric field distributions of the sample were calculated by thin film design software and are shown in Fig. 4.

The damage of materials can be explained by the excitation of electrons from the valence band (VB) to the conduction band (CB) via processes such as avalanche ionization (AI) and photoionization (PI)[10]. The laser-induced defect can be reversible or irreversible. The native absorbing defects and irreversible laser-induced defects were considered as trapping states[11] in order to explain the accumulation effects in 355 HR coatings in the model. In our calculation, the multiphoton ionization and impact ionization only produced the seed electrons, and these seed electrons achieved the critical plasma density through absorbing defects. The simplest energy diagram is illustrated in Fig. 5. Once in the CB, electrons

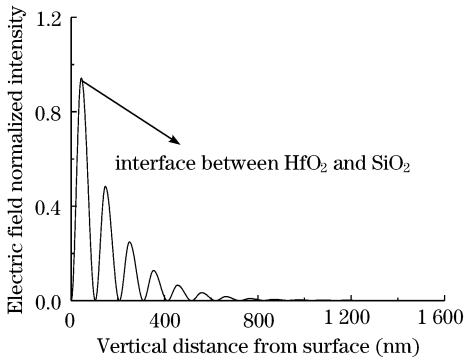

Fig. 4. Electric field intensity profile in HfO_2/SiO_2 HR coatings normalized to the incident electric field value at wavelength of 355 nm.

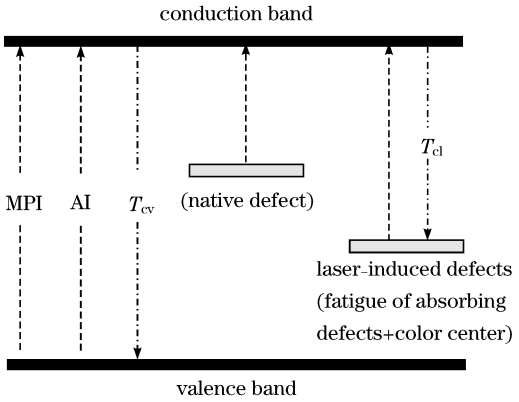

Fig. 5. Energy-level diagram of coatings.

can relax to the VB with a characteristic time constant T_{cv}. The defect trapping rate of electrons from the CB is characterized by a time constant T_{cl}.

The electron density (ED) in the CB is described by the following set of rate equation:

$$\frac{dn}{dt} = W_{AV}n(t) + W_{PI} + \sigma_{nd}n(t)I(t) - \frac{n(t)}{T_{cv}} + \sigma_{ld}n_{ld}(t)I(t) - \frac{n(t)}{T_{cl}}\left[1 - \frac{n_{ld}(t)}{n_{ld,max}}\right], \quad (1)$$

where W_{AV} and W_{PI} are the AI and PI rates, respectively; n_{ld} is the number densities of laser-induced defects; σ_{nd} is the absorption cross section of the native defects; and σ_{ld} is the absorption cross section of the laser-induced defects. The AI rate W_{AV} is calculated by the Drude model[12]:

$$W_{AV} = \frac{\sigma}{E_g}I(t), \quad (2)$$

where $\sigma = \frac{e^2}{c\varepsilon_0 n_0 m^*} \cdot \frac{\tau_c}{1 + w^2\tau_c^2}$ is the absorption cross section; e denotes the electron charge; $\tau_c = \frac{16\pi\varepsilon_0^2\sqrt{m^*(0.1E_g)^3}}{\sqrt{2}e^4 n(t)}$ is the resulting collision time, which is reciprocal to the ED; and E_g is the intrinsic material gap. $I(t)$ is the laser intensity, which is given by $I(t) = I_0 \exp(-4\ln 2t^2/\tau^2)$, where I_0 is the laser fluence

Table 1. List of Parameters for HfO_2 and SiO_2

	E_g (eV)	n_0	m^*	$m_e = m_h$
HfO_2	5.6	1.93	0.635	1.0
SiO_2	7.8	1.43	0.635	1.0

Values for E_g are obtained from Ref. [15]. The values for m^*, m_e, and m_h are obtained from Ref. [16].

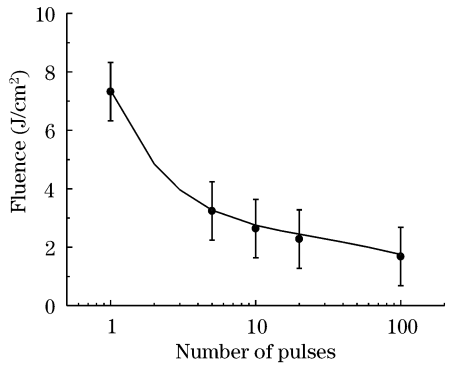

Fig. 6. Multi-shot LIDT of the sample; the solid lines are simulations from the model.

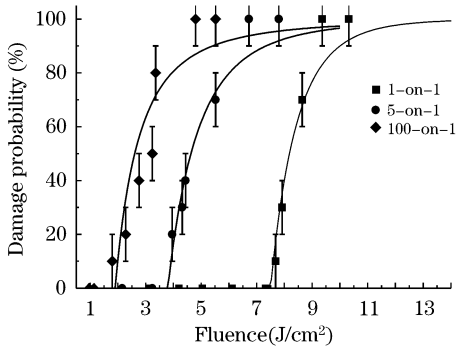

Fig. 7. Laser damage probability curves after 1, 5, and 100 shots, respectively.

and τ is the pulse duration. In the case of low electric fields, the PI rate describes the probability for multiphoton ionization (MPI); the PI rate can be described by the Keldysh's PI rate theory, which is most commonly used to calculate the excitation rate of electrons[13]:

$$W_{\text{multpt}} = \frac{2w}{9\pi}\left(\frac{m^* w}{\hbar}\right)^{3/2}\Phi\left[\left(\sqrt{2\left\langle E'_g/\hbar w\right\rangle - 2E'_g/\hbar w}\right)\right] \times \exp\left\{2\left\langle E'_g/\hbar w\right\rangle\left(1-\frac{1}{4\gamma^2}\right)\right\}\left(\frac{1}{16\gamma^2}\right)^{\left\langle E'_g/\hbar w+1\right\rangle}, \quad (3)$$

where $\gamma = w\sqrt{m_e^* E_g}/eE$; E is the electric field oscillating at frequency w; $E'_g = E_g\left[1+(1/2\gamma^2)\right]$ represents the effective band gap energy in the radiation field; $m^* = m_e m_h/(m_e+m_h)$ indicates the reduced effective mass of the conduction electron and valence hole; m_h is the effective conductivity masses of holes; the symbol $\langle\cdot\rangle$ denotes the integer part; and Φ describes the Dawson function.

The ED in the laser-induced defects is given by the following set of rate equation[14]:

$$\frac{dn_{ld}}{dt} = \frac{n(t)}{T_{cl}}\left[1-\frac{n_{ld}(t)}{n_{ld,max}}\right] - \sigma_{ld} n_{ld}(t) I(t), \quad (4)$$

where $n_{ld,max}$ is the maximum laser-induced defects density.

Between the pulses, the laser intensity is zero. When the CB ED surpasses a critical plasma density n_{cr}, the damage will occur. The quantities $n_{ld,max}$ and σ_{ld} were adjusted to match the experiment.

When the ED in the CB reaches a critical ED n_{cr} considered generally as the damage criterion, the materials absorb strongly through the process of inverse bremsstrahlung, resulting in reversible or irreversible changes, which is represented by[12] $n_{cr} = \frac{\varepsilon_0 m^* w^2}{e^2}$, where m^* is the effective conductivity masses of electrons, w is the incident laser frequency.

The band gaps of bulk materials SiO_2 and HfO_2 are 7.8 and 5.6 eV[15], respectively. The damage would likely occur in the SiO_2 protective layer first, thus the parameters of SiO_2 were used in our calculation. The values for all parameters in Eqs. (1)−(4) are shown in Table 1. The parameters used in the calculation are $n_{ld,max} = 2\times10^{19}$ cm^{-3} and $\sigma_{ld} = 1.8\times10^{-4}$ cm^2/J. The values were taken from the best fits to experiments from the samples. The equations were solved numerically, and the simulated result is shown in Fig. 6.

Considering the surface defects under Gaussian illumination, the damage probability can be expressed as[17]

$$p(F) = 1 - \exp[-dS_T(F)], \quad (5)$$

where d is the surface density of the defects and S_T is the part of the spot size where the energy density is greater than the precursor threshold T. Surface S_T is given by

$$S_T = 0.5S\ln(F/T), \quad (6)$$

where $S = \pi L^2$ is the spot size defined at $1/e^2$ and L is the radius obtained at $1/e^2$. The probability law that results from the relation of Eqs. (5) and (6) can be written as

$$p(F) = 1 - (F/T)^{-dS/2}. \quad (7)$$

Figure 7 gives the experiment data for the irradiation of 1-on-1, 5-on-1, and 100-on-1, respectively. With the model mentioned above, we have obtained a good agreement between the experiment data and the numerical simulation with error. The following parameters were used in the calculation: $d_{1-on-1} = 320$ defects/mm^2, $d_{5-on-1} = 140$ defects/mm^2, and $d_{100-on-1} = 90$ defects/mm^2. This result indicates that the creation of laser-induced defects is involved in the multi-shot damage. This means that when the coating is at a certain laser radiation below the 1-on-1 LIDT, the damage will occur because of the accumulation of the irreversible laser-induced defects in the multi-shot procedure.

In conclusion, the native defects and laser-induced defects will play a role in multi-shot damage. The multi-shot LIDT being lower than single-shot LIDT is related to the accumulation of laser-induced defects. A model that includes native defects and laser-induced defects is developed for multi-shot damage in wide gap dielectric materials.

References

1. S. C. Jones, P. Braunlich, R. T. Casper, X. A. Shen, and P. Kelly, Opt. Eng. **28,** 1039 (1989).
2. A. A. Manenkov and V. S. Nechitailo, in *Proceedings of Laser-Induced Damage in Optical Material* 392 (1991).
3. J. Y. Natoli, B. Bertussi, and M. Commandre, Opt. Lett. **30,** 1315 (2005).
4. F. R. Wagner, A. Hildenbrand, L. Gallais, H. Akhouayri, M. Commandre, and J. Y. Natoli, Proc. SPIE **7132,** 71320Y (2008).
5. X. Li, Y. Zhao, X. Liu, J. Shao, and Z. Fan, Chin. Opt. Lett. **8,** 615 (2010).
6. L. A. Emmert, M. Mero, and W. Rudolph, J. Appl. Phys. **108,** 043523 (2010).
7. Y. Wang, H. He, Y. Zhao, Y. Shan, D. Li, and C. Wei, Chin. Opt. Lett. **9,** 023013 (2011).
8. L. A. Siiman and L. B. Glebov, in *Proceedings of Laser-Induced Damage in Optical Materials* **5991,** 99112 (2005).
9. ISO11254-2, "Lasers and laser-related equipment-determination of laser -induced damage threshold of optical surfaces-Part 2" in *s-on-1 test* (2000).
10. N. Bloembergen, IEEE J. Quantum Electron. **10,** 375 (1974).
11. M. Mero, L. A. Emmert, and W. Rudolph, Proc. SPIE **7132,** 713209 (2008).
12. K. Starke, D. Ristau, H. Welling, T. V. Amotchkina, M. Trubetskov, A. A. Tikhonravov, and A. S. Chirkin, Proc. SPIE **5273,** 501 (2004).
13. L. V. Keldysh, Sov. Phys. JETP **20,** 1307 (1965).
14. M. Mero, B. Clapp, J. C. Jasapara, W. Rudolph, D. Ristau, K. Starke, J. Kruger, S. Martin, and W. Kautek, Opt. Eng. **44,** 051107 (2005).
15. L. Yuan, Y. N. Zhao, G. Q. Shang, C. R. Wang, H. B. He, J. D. Shao, and Z. X. Fan, J. Opt. Soc. Am. B **24,** 538 (2007).
16. L. Sudrie, A. Couairon, M. Franco, B. Lamouroux, B. Prade, S. Tzortzakis, and A. Mysyrowicz, Phys. Rev. Lett. **89,** 186601/1 (2002).
17. J. Y. Natoli, L. Gallais, H. Akhouayri, and C. Amra, Appl. Opt. **41,** 3156 (2002).